ARTICLE

BIOTECHNOLOGY and BIOENGINEERING

Manufacturing of Bioreactive Nanofibers for Bioremediation

Ho-Wang Tong,[1] Baris R. Mutlu,[1] Lawrence P. Wackett,[2,3] Alptekin Aksan[1,2]

[1]Department of Mechanical Engineering, University of Minnesota, 111 Church St. SE, Minneapolis, Minnesota 55455; telephone: +1-612-626-6618; fax: +1-612-626-1854; e-mail: aaksan@umn.edu

[2]The BioTechnology Institute, University of Minnesota, Saint Paul, Minnesota 55108

[3]Department of Biochemistry, Molecular Biology and Biophysics, University of Minnesota, Minneapolis, Minnesota

ABSTRACT: Recombinant *Escherichia coli* (*E. coli*) cells were successfully encapsulated in reactive membranes comprised of electrospun nanofibers that have biocompatible polyvinyl alcohol (PVA)-based cores entrapping the *E. coli* and silica-based, mechanically sturdy porous shells. The reactive membranes were produced in a continuous fashion using a coaxial electrospinning system coupled to a microfluidic timer that mixed and regulated the reaction time of the silica precursor and the PVA solution streams. A factorial design method was employed to investigate the effects of the three critical design parameters of the system (the flow rate of the core solution, protrusion of the core needle, and the viscosity of the core solution) and to optimize these parameters for reproducibly and continuously producing high-quality core/shell nanofibers. The feasibility of using the reactive membranes manufactured in this fashion for bioremediation of atrazine, a herbicide, was also investigated. The atrazine degradation rate (0.24 μmol/g of *E. coli*/min) of the encapsulated *E. coli* cells expressing the atrazine-dechlorinating enzyme AtzA was measured to be relatively close to that measured with the free cells in solution (0.64 μmol/g of *E. coli*/min). We show here that the low cost, high flexibility, water insolubility, and high degradation efficiency of the bioreactive membranes manufactured with electrospinning makes it feasible for their wide-spread use in industrial scale bioremediation of contaminated waters.

Biotechnol. Bioeng. 2014;111: 1483–1493.

Correspondence to: A. Aksan

Contract grant sponsor: NSF-IIP/PFI
Contract grant number: #1237754
Contract grant sponsor: NSF-CAREER
Contract grant number: #0644784
Contract grant sponsor: BioTechnology Institute and the College of Biological Sciences in University of Minnesota
Received 17 August 2013; Revision received 25 January 2014; Accepted 29 January 2014
Accepted manuscript online 6 February 2014;
Article first published online 24 February 2014 in Wiley Online Library (http://onlinelibrary.wiley.com/doi/10.1002/bit.25208/abstract).
DOI 10.1002/bit.25208

KEYWORDS: bioremediation; atrazine; bioencapsulation; bacteria; silica; electrospinning

Introduction

More than one-third of the accessible freshwater throughout the world is used for agricultural, industrial, and domestic purposes, leading to worldwide contamination of freshwater systems with myriads of chemicals such as pesticides (e.g., DDT, acetochlor, and atrazine) or heavy metals (e.g., lead, mercury, and cadmium) as well as various synthetic chemicals, unmetabolized drugs, hydrocarbons and radioactive wastes affecting the health of billions of people. In this context, contamination of waters has become one of the major problems facing humanity and this issue has received considerable attention over the past two decades (Guillette and Iguchi, 2012; Schwarzenbach et al., 2006).

Electrospun membranes has been widely used in traditional filtration, and manufacturing of biosensors, protective clothing, energy conversion systems, cosmetics, tissue engineering products, drug delivery systems, electronic and optical devices, food items, and advanced composite materials (Bhardwaj and Kundu, 2010; Lopez-Rubio et al., 2012; Miao et al., 2010; Zucchelli et al., 2011). Thanks to their high permeability, small pore size, high specific surface area, good interconnectivity of pores and ability to be functionalized chemically at the nanoscale, electrospun nanofibrous membranes have been used in environmental remediation applications for the removal of different contaminants from wastewaters such as adsorption of heavy metal ions (Abbasizadeh et al., 2013; Irani et al., 2012; Li et al., 2011; Ma et al., 2011; Mahapatra et al., 2012; Wang and Ge, 2013). Apart from their adsorbtive capability (e.g., of heavy metal ions), electrospun nanofibrous membranes are also suitable candidates for biodegradation of various

contaminants because of their potential to incorporate immobilized enzymes (Wang et al., 2009) or encapsulate cells within (Zussman, 2011). Dai et al. (2013) and Niu et al. (2013a) made laccase-containing fibrous mats by emulsion electrospinning and have reported rapid adsorption and degradation of polycyclic aromatic hydrocarbons. Similarly, horseradish peroxidase (HRP)-containing fibrous mats were made by emulsion electrospinning and the adsorption and degradation of pentachlorophenol (PCP) was measured (Niu et al., 2013b). The PCP adsorption values reached were as high as 44.69 mg/g while the removal efficiencies were 83% and 47% for the immobilized and the free HRP, respectively. Singh et al. (2013) used electrospun ZnO nanofibrous mats and demonstrated the efficacy of these mats in complete degradation of naphthalene and anthracene dyes in waters. In a recent study, Klein et al. (2012) encapsulated *Pseudomonas* sp. ADP cells into electrospun microfibers and demonstrated their atrazine degradation ability.

There are significant advantages offered by reactive filtration systems and biosensors that utilize bioreactive organisms encapsulated in electrospun microfibers. There is also the potential for wide-spread industrial use due to very high surface area to volume ratio achieved, ease in scale up and the cost-effectiveness of the technology. However, development of a water insoluble, solvent-free and multilayered coaxial encapsulation technology that ensures long-term reactivity of the encapsulated microorganisms remains to be a challenge. Figure 1 summarizes the critical requirements for wide-spread adoption of encapsulated cell-based electrospun systems in bioremediation industry. In previous studies to date, cells have been encapsulated into electrospun nanofibers made of materials that slowly degrade, such as polycaprolactone (PCL) (Klein et al., 2009), or are not biodegradable, such as Pluronic F127 dimethacrylate (FDMA) (Liu et al., 2009). However, these fabrication processes required extensive use of organic solvents, which are known to reduce the reactivity and longevity of the encapsulated cells. Electrospinning techniques that do not require the use of organic solvents were also developed and live cells have successfully been encapsulated by electrospinning (Fung et al., 2011; Gensheimer et al., 2007; Lopez-Rubio et al., 2009; Salalha et al., 2006). However, the resultant materials were water-soluble, making them unsuitable for use in aqueous environments that are encountered in all water bioremediation applications.

Silica nanofibers can be made by sol–gel electrospinning without using organic solvents, and the produced electrospun nanofibers are water-insoluble (Kim et al., 2010; Patel et al., 2006). This makes silica an appealing material for electrospin encapsulation biological materials, but the electrospinning process is not stable due to continuously changing viscosity of the silica precursor solution during gelation (Ponton et al., 2002). In the present study, we developed an electrospinning system that utilizes a microfluidic timer coupled with a coaxial electrospinning setup. We utilized coaxial electrospinning that combines a silica

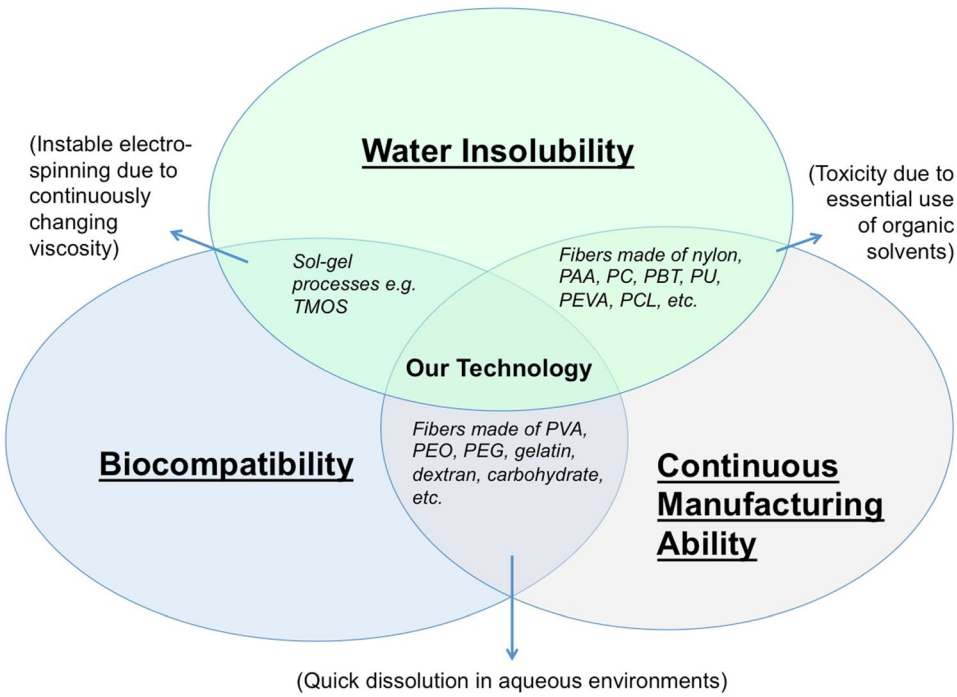

Figure 1. Critical requirements for electrospinning reactive bacteria for bioremediation applications.

precursor solution (that formed a hard shell around the nanofibers) and a bacteria suspension medium (that formed the biocompatible core for the nanofibers, encapsulating reactive bacteria). This enabled us to continuously produce water insoluble, high bioreactivity nanofibers thus satisfying the critical design requirements for successful bioremediation applications (Fig. 1).

Materials and Methods

Materials

Tetramethyl orthosilicate (TMOS), hydrochloric acid (HCl), and polyvinyl alcohol (PVA) were obtained from Sigma (Sigma–Aldrich Corp., St. Louis, MO). Eight percent to 28% (w/v) PVA was dissolved in water to make the core solution. Silica was used as the shell solution by hydrolyzing TMOS in the presence of HCl. The molar ratio of TMOS:water:HCl was 1:2.8:0.00024. *E. coli* expressing green fluorescent protein (GFP) were encapsulated for confocal microscopy imaging while the *E. coli* expressing atrazine chlorohydrolase (AtzA) were encapsulated to be used for atrazine bioremediation activity assays (Strong et al., 2000).

Preparation of Reactive Membranes

Figure 2 shows the schematic of the designed electrospinning setup capable of forming reactive membranes comprised of nanofibers that have PVA-based biocompatible cores that contain the encapsulated bacteria and porous silica shells surrounding the core. To prepare the core solution, *E. coli* pellets were mixed with the PVA solution at a cell loading density of 0.5 g/mL and the mixture was loaded into syringe A. Three different PVA solution concentrations (8%, 18%, and 28%, w/v) were investigated. The hydrolyzed TMOS solution was loaded into syringe B, which was connected to one of the inlets of a microfluidic timer. The 18% (w/v) PVA solution, which had the optimum viscosity for electrospinning when mixed with the TMOS solution, was loaded into syringe C, which was connected to the other inlet of the microfluidic timer. The microfluidic timer precisely controlled the reaction of the hydrolyzed TMOS solution and the 18% (w/v) PVA solution. The reaction time was set to 9 min to ensure that the optimum viscosity of the mixture is reached during gelation before electrospinning. The viscosities of the shell solution and the core solutions at different PVA concentrations were measured by a digital viscometer (NDJ-8S, Shanghai Nirun Intelligent Technology Co Ltd., Shanghai, China). The flow rates of the shell TMOS solution extruded from syringe B and the PVA solution fed from syringe C were 0.7 and 0.5 mL/h, respectively. This was done to reach an optimum viscosity value for the mixture. A voltage of 15 kV was applied to the outer needle by a high voltage power supply so that the shell solution was drawn by the electric force while the core solution was drawn by the shear force at the interface of the core solution and the shell solution, as illustrated in Figure 2c. Core/shell structured nanofibers were collected by a grounded conductive plate. As a control, core/shell nanofibers that do not contain any bacteria were manufactured.

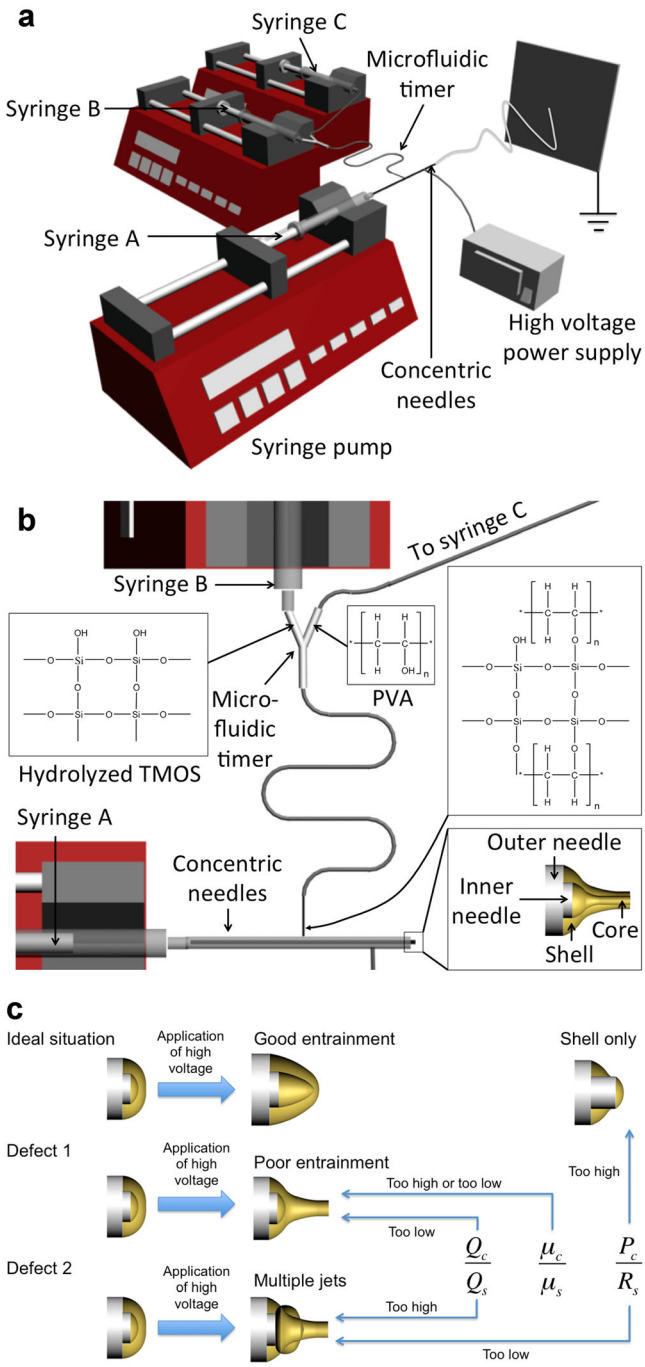

Figure 2. Electrospinning setup for core/shell nanofibers that have a bacterium-containing PVA core and a silica-based shell surrounding the core: (**a**) The coaxial electrospinning system that is coupled to a microfluidic timer; (**b**) The chemical reaction between the hydroxide groups of PVA and the silanol groups of silica during the electrospinning process; (**c**) The effects of the three critical parameters: The ratio of the core solution flow rate to the shell solution flow rate (Q_c/Q_s), the ratio of the core needle protrusion length to the shell needle radius (P_c/R_s), and the ratio of the viscosity of the core solution to the viscosity of the shell solution (μ_c/μ_s).

Optimization of Parameters

The quality of the electrospinning manufacturing system is defined by cell encapsulation efficiency (g cells encapsulated per g material produced), and the production homogeneity (minimization of defects such as droplets intermixed with the fibers as well as ensuring a uniform diameter distribution of the nanofibers). Therefore, the quality of the product is affected by the physical and chemical properties of the solutions used to make the core and the shell as well as the processing parameters. To achieve the highest quality for production, a factorial design method was employed to optimize the solution properties and the processing parameters.

Selection of the Manufacturing Parameters

Continuous manufacturing of core/shell nanofibers via coaxial electrospinning relies on the formation of a jet of the shell solution and the entrainment of the core solution. For successful entrainment of the core solution, certain parameters should be optimized: (1) ratio of the flow rate of the core solution to the flow rate of the shell solution (Q_c/Q_s), (2) ratio of the core needle protrusion to the outer needle radius (P_c/R_s), and (3) ratio of the viscosity of the core solution to the viscosity of the shell solution (μ_c/μ_s) (Reznik et al., 2006). The effect of these parameters on coaxial electrospinning is illustrated in Figure 2c. Extreme values of these ratios generally lead to poor entrainment of the core material into the jet or formation of multiple jets rather than a stable core/shell jet (Moghe and Gupta, 2008). The values/levels for the parameters investigated in the present study are listed in Table I. Level 0, level 1, and level 2 corresponded to the low, medium and high levels, respectively. A complete factorial design with three parameters and three levels was constructed to estimate the resultant effects and the interactions between these parameters to determine the best conditions to continuously produce core/shell nanofibers (Table II).

Product Quality Estimation

To determine the quality of the reactive membranes, three aspects should be considered: cell encapsulation efficiency (y_1), droplet (defect) formation (y_2), and fiber diameter (y_3). An ideal reactive membrane should have a large density of encapsulated cells to enhance its specific degradation rate per volume of the material produced. The defects (i.e., droplets) should be minimized so that additional processes/steps for the removal of the defects from the final product are not needed. Uniform fibers with smaller diameters are preferred because they not only decrease diffusion length when the fiber diameter is larger than the bacteria size but also result in a higher surface area-to-volume ratio and permeability.

Table I. Parameters and levels investigated in the factorial design.

	Level		
Parameter	0	1	2
A. Core solution flow rate (mL/h)	0.6	1.2	1.8
B. Core needle protrusion length (mm)	0.2	0.4	0.6
C. Core solution concentration (%, w/v)	8.0	18.0	28.0

To determine the cell encapsulation efficiency, *E. coli* expressing GFP were encapsulated in electrospun reactive membranes. The membranes were then washed with ultrapure water three times to get rid of the loosely bound, surface-attached cells to ensure that only fully encapsulated cells are visualized in the subsequent confocal microscopy images (Olympus FluoView FV1000, Center Valley, PA). For each membrane, confocal microscopy images were obtained at three different regions (the area of each region was $0.01\,mm^2$). The number of cells in each region was counted (using green fluorescence imaging). The average value (N_c), which reflected the number of cells within an area of $0.01\,mm^2$, was used as a measure of cell encapsulation efficiency. The cell encapsulation efficiency of each sample was given a value (y_1), normalized with respect to the maximum number of cells (N_{cmax}) measured among all samples so that y_1 values were kept in a range between 0 and 1 (Eq. 1). As the number of cells in Exp. 3 was the maximum among all samples, N_c was taken to be equal to N_{cmax} in Exp. 3. Therefore, $y_1 = 0$ in Exp. 3, as can be seen in Table II

$$y_1 = \frac{N_{cmax} - N_c}{N_{cmax}} \tag{1}$$

To determine defect formation, each reactive membrane sample was examined by scanning electron microscopy (SEM) (Hitachi S-4700, Tokyo, Japan). In each sample, SEM micrographs were obtained at three different regions measuring approximately $256\,\mu m^2$. The number of droplets (that are not connected to fibers) in each region was counted and the values determined at the three regions were averaged (N_d). The defect formation in each sample was given a value (y_2) and normalized with respect to the maximum number of droplets (N_{dmax}) measured among all samples so that y_2 fell within a range between 0 and 1 (Eq. 2). As the number of droplets in Exp. 19 was the maximum among all samples, N_d was equated to N_{dmax} in Exp. 19. Therefore, $y_2 = 1$ in Exp. 19, as can be seen in Table II

$$y_2 = \frac{N_d}{N_{dmax}} \tag{2}$$

To determine the fiber diameter uniformity in the produced filters, each SEM micrograph was analyzed using ImageJ. The fiber diameters were measured at 50 different locations and the average fiber diameter (D) was obtained. The response reflecting the fiber diameter of each sample was given a value (y_3) and normalized with respect to the maximum fiber diameter (D_{max}) to ensure that y_3 fell within a range between 0 and 1 (Eq. 3). As the fiber diameter in Exp. 12 was the maximum among all samples, D was taken as D_{max}

Table II. Effects of the three chosen parameters on the quality (y) of the electrospun fibers.

	Parameter and its level						
Exp.	A	B	C	Response y_1	Response y_2	Response y_3	Overall response y
1	0	0	0	0.7810	0.3088	0.6026	0.5641
2	0	0	1	0.5429	0.1324	0.6485	0.4412
3	0	0	2	0	0	0.8603	0.2868
4	0	1	0	0.6571	0.3235	0.5993	0.5267
5	0	1	1	0.3048	0.2353	0.6648	0.4016
6	0	1	2	0.3048	0	0.6714	0.3254
7	0	2	0	0.9714	0	0.6616	0.5443
8	0	2	1	0.9810	0	0.7194	0.5668
9	0	2	2	0.9905	0	0.7194	0.5700
10	1	0	0	0.6381	0.5735	0.5819	0.5978
11	1	0	1	0.4857	0.3676	0.7784	0.5439
12	1	0	2	0.2667	0	1	0.4222
13	1	1	0	0.6476	0.5735	0.5742	0.5985
14	1	1	1	0.5143	0.4265	0.7707	0.5705
15	1	1	2	0.3048	0	0.9662	0.4236
16	1	2	0	0.9905	0	0.6572	0.5492
17	1	2	1	0.9810	0	0.7151	0.5653
18	1	2	2	0.9810	0	0.7271	0.5693
19	2	0	0	0.5524	1	0.5448	0.6990
20	2	0	1	0.2952	0.7353	0.6343	0.5549
21	2	0	2	0.1714	0	0.9651	0.3788
22	2	1	0	0.2952	0.4853	0.5699	0.4501
23	2	1	1	0.2476	0.1471	0.6288	0.3412
24	2	1	2	0.0762	0	0.9727	0.3496
25	2	2	0	0.9714	0	0.6703	0.5472
26	2	2	1	0.9905	0	0.7205	0.5703
27	2	2	2	0.9905	0	0.7194	0.5700

in Exp. 12. Therefore, $y_3 = 1$ in Exp. 12, as can be seen in Table II

$$y_3 = \frac{D}{D_{\max}} \tag{3}$$

The overall response (y) that corresponds to the overall quality of the manufactured filter (Eq. 4) is calculated as the weighted average of all of the parameters measured above

$$y = \frac{y_1 + y_2 + y_3}{3} \tag{4}$$

The weight for each outcome (y_i) can be adjusted according to the desired application. If a very high atrazine degradation efficiency is desired at the expense of increased defects (i.e., a high number of droplets with respect to the number of fibers) in the finished product, one may assign a higher weight for cell encapsulation efficiency and a lower weight for tendency of droplet formation. On the contrary, if a moderately high atrazine degradation efficiency is sufficient but the homogeneity of the finished product is of utmost concern, one may assign a higher weight for the defect formation and a lower weight for the cell encapsulation efficiency. In this manuscript, we assigned equal weights to each of the three outcomes (y_i) used in this study.

The value of overall response (y) was between 0 and 1 for each reactive membrane manufactured in this study. A quality response value of 0 indicated that the reactive membrane had a high amount of encapsulated cells, had minimum defects, and the smallest fiber diameter among all reactive membranes investigated, whereas a value of 1 meant the opposite. A reactive membrane with the minimum overall response was regarded as the optimized membrane. The 27 experimental conditions conducted in the three-parameter, three-level factorial design and the corresponding overall responses were analyzed by a statistical analysis software (Statgraphics®) and optimum values for operational parameters were determined.

Characterization

Fourier transform infrared spectroscopy (FTIR) analysis was conducted with the reactive membranes manufactured using the optimized parameters, silica/PVA nanofibrous membranes that did not contain any bacteria, and silica/PVA mixtures with known *E. coli* content (for calibration) using a Nicolet Continuμm FTIR microscope. IR spectra in the range of 400–4,000 cm^{-1} were recorded at a resolution of 4 cm^{-1}. Each sample was scanned at five different regions on the sample using an aperture size of 100 μm × 100 μm. The amount of the encapsulated *E. coli* in the electrospun membrane sample was calculated using the ratio of the intensity of the Amide II peak (corresponding to cellular proteins) to the intensity of the methylene peak (originating from silica and PVA) (Fig. S1).

For SEM and Transmission Electron Microscopy (TEM, FEI Tecnai G^2 F30, Hillsboro, OR) imaging, reactive membranes containing *E. coli* cells expressing AtzA were manufactured using the optimized values for the parameters examined. Reactive membranes comprised of core/shell nanofibers without any bacteria were also fabricated in a similar fashion.

Biotransformation of Atrazine Into Hydroxyatrazine

Activity measurements of the optimized reactive membranes were conducted at room temperature. The reaction was initiated by exposing the optimized reactive membrane to 5 mL of 0.1 M potassium phosphate buffer (at pH 7.0) containing 150 μM (32.4 ppm) atrazine. The supernatant was sampled after 20 min and the concentrations of atrazine and its metabolite, hydroxyatrazine, were measured by high-performance liquid chromatography (HPLC) as previously described (de Souza et al., 1995). Activity measurements of the free bacteria were conducted in a similar fashion.

Results and Discussion

Fabrication of Silica-PVA-Based Core/Shell Encapsulating Nanofibers

Silica is an excellent material for bioencapsulation because of its low cost, mechanical robustness, manufacturability, thermal and pH stability, and chemical inertness (Nassif et al., 2002). Unlike most electrospun fibers, especially those made of natural polymers such as gelatin or alginate, which are mechanically fragile and rapidly dissolve in water, silica fibers can maintain their morphology in water during continuous use. Nevertheless, the silica fibers are yet quite brittle. Fabrication of silica nanofibers via traditional electrospinning methods has previously been reported (Shin et al., 2010; Tsou et al., 2008). For example, tetraethyl orthosilicate (TEOS) has widely been used for fabricating pure silica or silica-polymer nanofibers via sol–gel electrospinning (Katoch and Kim, 2012; Pirzada et al., 2012). However, the sol–gel process unavoidably requires ethanol, which is not only released by the hydrolysis reaction but also is added to eliminate phase separation and to accelerate hydrolysis. However, ethanol is known to negatively affect the reactivity and the viability of the encapsulated bacteria. Therefore, to date there has been no report of successful encapsulation of reactive bacteria in electrospun silica nanofibers. A mixture of TEOS and aminopropyl triethoxysilane (APTES) (Irani et al., 2012) has also been used for forming silica nanofibers via sol–gel electrospinning but the process still requires ethanol.

In this communication, reactive membranes comprised of nanofibers made of silica and PVA were produced using a novel coaxial electrospinning process. The uniqueness of the approach presented here is that no extra ethanol needed to be added during the process, which maximized the biocompatibility of the produced material while enabling continuous production. Furthermore, the technology aims at encapsulation of intact bacteria, not purified enzymes. The advantage of encapsulating bacteria over enzymes is that it is easier and more economical to grow and use bacteria as the biodegradation agent since additional steps for enzyme purification are not required. Furthermore, in intact cell encapsulation, the enzymes are better protected against swings in temperature, pH, and salinity since they reside in their native environment in the cytoplasm of the cells.

Polyvinyl alcohol (PVA) used in the formulation served multiple purposes; (1) PVA acted as a thickener, helping to adjust the viscosity of the electrospinning solution, (2) enhanced biocompatibility of the bioencapsulation solution by enveloping and protecting the bacteria from the gelling silica precursors, (3) when mixed with the silica in the shell solution, decreased the brittleness of the shell and increased its flexibility, (4) Increased the porosity of the shell, and (5) dissolved away when the finished product was exposed to an aqueous solution, therefore increasing the permeability of the membrane (Fig. 3a).

Optimization of Electrospinning Parameters

The quality of the electrospun reactive membrane (represented by the overall response, y) is a function of three parameters: cell loading density (represented by the response y_1), defect formation (represented by the response y_2), and uniformity of the produced fiber diameters (represented by the response y_3). The value y was taken to be the average of y_1, y_2, and y_3 and the lower the value of y, the higher the quality of the produced reactive membrane. The value y for each formulation was determined and is summarized in Table II. It can be clearly seen that the overall response y reached the minimum at Experimental condition 3, corresponding to the optimum design conditions for manufacturing of the reactive membranes. On the contrary, the overall response y was the highest at Experimental condition 19, indicating that the combination of the design parameters resulted in a sub-standard membrane material.

Figure 3 shows the SEM micrographs of the reactive membranes that contain GFP expressing *E. coli* encapsulated at conditions corresponding to Exp. 3 (Fig. 3b) and Exp. 19 (Fig. 3c). The inserts show the confocal microscopic images of the same samples. It can be clearly seen that more cells were encapsulated in Exp. 3 compared to Exp. 19. This could be explained by rheological analysis: The viscosity of the core solution used in Exp. 3 was approximately 4,000 cP while it was below 1,000 cP in Exp. 19. The viscosity of the shell solution, identical in both cases, was measured to be $4{,}173 \pm 686$ cP, a value very similar to the viscosity of the core solution in Exp. 3, but significantly higher than that in Exp. 19. Therefore, it was easier for the core at Exp. 3 to be entrained by the shell solution and incorporated into the electrospun jet by the shear force generated at the core–shell interface, thus enhancing the cell encapsulation efficiency. Although the average diameter of the fibers fabricated at Exp. 19 was slightly smaller than that at Exp. 3, the membranes fabricated at Exp. 19 were not considered to be superior than

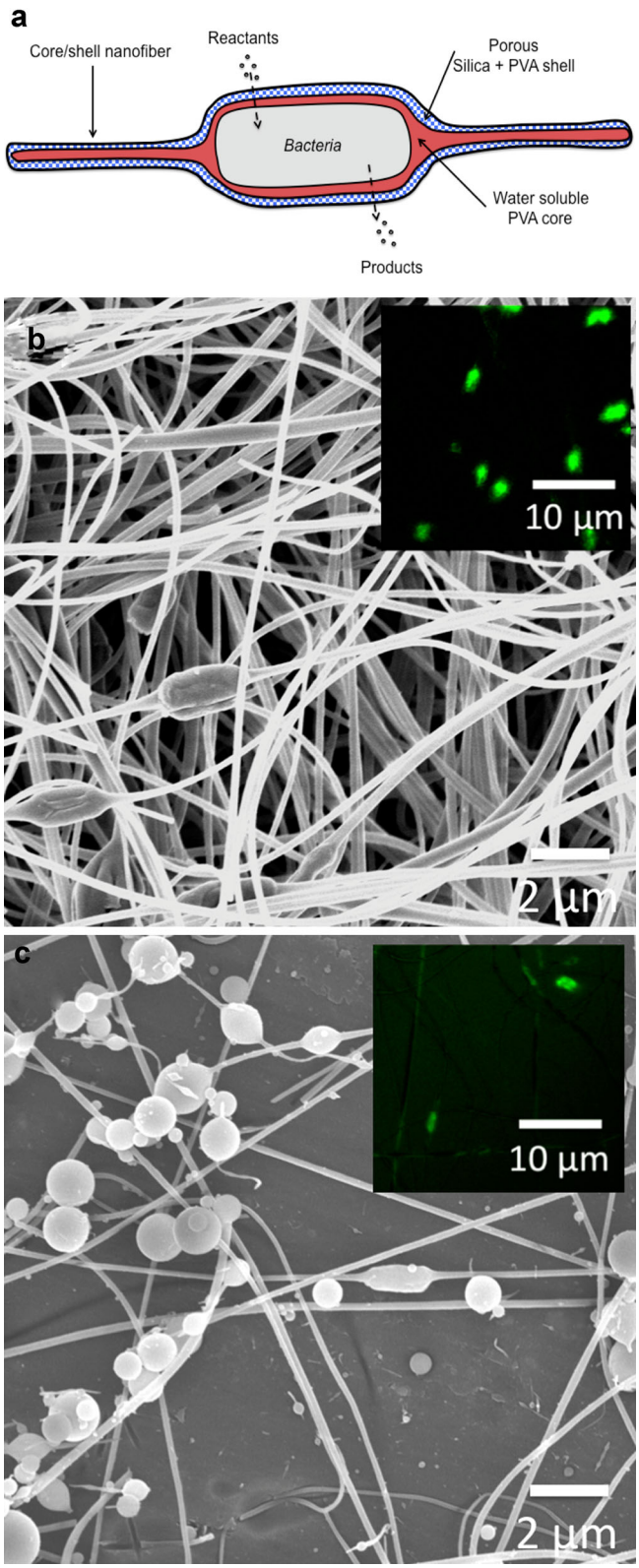

Figure 3. **a**: The nanofiber architecture comprised of a bacterium encapsulated in a water soluble PVA core and a silica-based porous shell surrounding the core. SEM micrographs and confocal microscopic images (insets) of the electrospun fibers that contain encapsulated *E. coli* expressing GFP: (**b**) Exp. 3; (**c**) Exp. 19.

those fabricated at Exp. 3 since the diffusional distance is independent of the fiber diameter when the fiber diameter is smaller than the width of the bacteria such that the thickness of the shell wall covering the bacteria remains unchanged. The diameters of the fibers in both samples were smaller than the width of an *E. coli* cell (around 500 nm). Therefore, the thickness of the encapsulating shell produced in Exp. 19 should be similar to that of the encapsulating shell is Exp. 3, even though the average fiber diameter in Exp. 19 was smaller. The substantial number of droplets observed in Exp. 19 results in a lower quality of the manufactured membranes. In Exp. 19, the core solution flow rate was high but the core solution was poorly entrained into the jet. Therefore, it is highly likely that the excess core solution is drawn as a separate jet, which might be broken down into droplets by the electric forces.

The main effects of core solution flow rate, core needle protrusion and core solution concentration on the overall response y were investigated. Figure 4a shows the surface plot as a function of the core solution flow rate and the core needle protrusion distance when the core solution concentration is kept constant at the medium level of 18% (w/v). The minimal response for y was observed when the core solution flow rate and the core needle protrusion were low, indicating that a high quality membrane could be manufactured by reducing both the core solution flow rate and the core needle protrusion. Figure 4b shows the response surface as a function of the core solution flow rate and the core solution concentration, with the core needle protrusion kept constant at the medium level (0.4 mm). The response, y, in general decreased with increasing core solution concentration but the core solution flow rate did not play a significant role, implying that for this specific protrusion length, a higher core solution concentration would result in a higher quality membrane. Figure 4c shows the response surface as a function of the core needle protrusion distance and the core solution concentration, when the core solution flow rate was kept constant at the medium level (1.2 mL/h). The minimum response for y was observed when core needle protrusion was at the low level while the core solution concentration was at the high level, indicating that the quality of the membrane could be increased by reducing the core needle protrusion and increasing the core solution concentration. Figure 4d shows the response plot as a function of all three parameters and the plot clearly indicates that the minimum response of y (corresponding to the highest quality of the membrane) could be achieved when the core solution flow rate and core needle protrusion were set to low while the core solution concentration was set to high. Therefore, the optimum parameters were chosen as: Core solution flow rate = 0.6 mL/h; core needle protrusion = 0.2 mm; and core solution concentration = 28%(w/v) for the production of the membranes to be characterized and analyzed in detail as described below.

Characterizations of the Optimized Reactive Membranes

E. coli-containing nanofibrous membranes fabricated under the optimized conditions were analyzed with FTIR

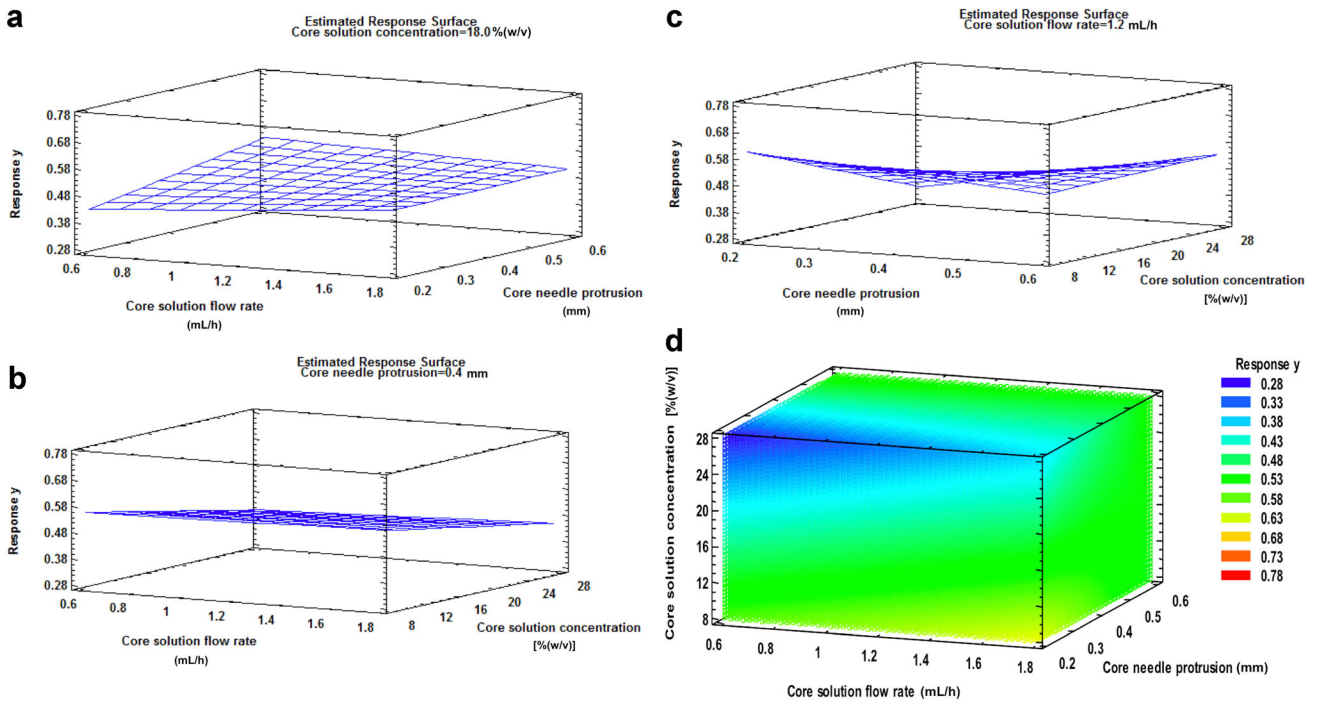

Figure 4. Three-dimensional response surface plots for the interactions between: (**a**) core solution flow rate and core needle protrusion; (**b**) core solution flow rate and core solution concentration; (**c**) core needle protrusion and core solution concentration; and (**d**) all three parameters.

spectroscopy. As shown in Figure S1, the silica/PVA matrix generated spectra with prominent peaks between 3,200 and 3,500 cm^{-1} originating from the ν-OH vibrations, the peaks between 2,900 and 3,000 cm^{-1} originating from the vibrations of the $–CH_2$ groups, the peaks around 1,430 cm^{-1} due to the scissoring motion of CH_2, and the peaks around 1,380 cm^{-1} due to the bending of CH_2. Apart from the aforementioned common peaks, the FTIR spectrum for the *E. coli*-containing nanofibrous membrane exhibited additional peaks including the peak at 1,656 cm^{-1} arising from the protein and water bending peaks generating the Amide I band and the peak at 1,542 cm^{-1} due to the Amide II protein band. The amount of *E. coli* encapsulated in the electrospun nanofibrous membranes was measured using the ratio of the intensity of the Amide II peak to the intensity of the CH_2 peak. In this analysis, the Amide II peak, instead of the Amide I peak, was used because the Amide II peak does not include spectral contributions from water bending peak located at 1,650 cm^{-1} (Pelton and McLean, 2000). Table III shows the correlation between the Amide II-to-CH_2 ratio (m) and the mass percentage of *E. coli* in fibers (n). The relationship between m and n was determined to be:

$$m = 0.1549\, e^{0.0473n} \quad (5)$$

Using this equation, the mass ratio of the *E. coli* in the electrospun reactive membranes produced at the optimum condition (Exp. 3) was determined as approximately 40% g cells/g matrix. This is a very high level of loading that has not been reported elsewhere before.

SEM imaging was used to explore the ultrastructure of the core/shell nanofibers fabricated at the optimized conditions (i.e., the conditions that minimized y). Figure 5a shows the electrospun membrane comprising the core/shell nanofibers. When encapsulated, the bacteria were oriented along the longitudinal direction of the nanofiber without experiencing a significant morphological change due to encapsulation (Fig. 5b). The surface of the nanofibers was smooth, indicating homogeneous mixing of the PVA with the silica. The average diameter of the AtzA expressing *E. coli*-containing nanofibers was 255 ± 19 nm, which was similar to that of the GFP expressing *E. coli*-containing nanofibers fabricated in Exp. 3 (263 ± 17 nm). The core/shell morphology of the nanofibers was confirmed by TEM imaging (Fig. 5c), which showed that the thickness of the porous silica shell was approximately 20 nm.

Table III. Relationship between the Amide II-to-CH_2 ratio (m) and the mass percentage of *E. coli* (n).

Mass percentage of *E. coli*, n (%, g/g)	Amide II-to-CH_2 ratio, m
36	0.8405 ± 0.0871
44	1.2659 ± 0.1146
51	1.7051 ± 0.1131

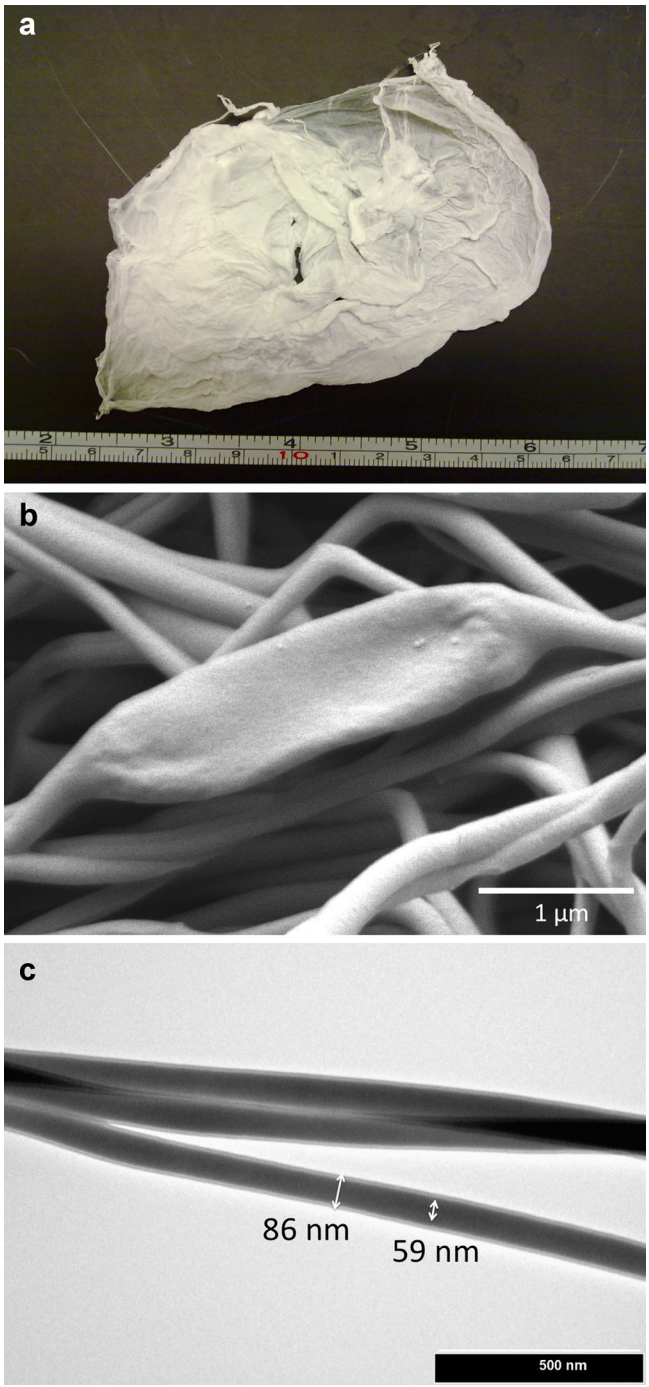

Figure 5. **a**: Core/shell nanofiber membranes produced by coaxial electrospinning with the optimized parameters, (**b**) SEM micrograph of the core/shell nanofibers showing an encapsulated *E. coli* (**c**) TEM image of the core/shell nanofibers showing the PVA core and a silica/PVA composite shell surrounding the PVA core (fiber portion between encapsulated bacteria was selected).

Biotransformation of Atrazine Into Hydroxyatrazine

Rietti-Shati et al. (1996) immobilized *Pseudomonas ADP* using Ca-alginate encapsulation technique and found that the bacterium lost much of its atrazine degrading activity upon immobilization (50% reduction in atrazine concentration before immobilization versus 8% reduction in atrazine concentration after immobilization). Vancov et al. encapsulated *Rhodococcus erythropolis* cells in alginate-based spherical beads and demonstrated the ability of the encapsulated cells to degrade atrazine. However, with soft materials such as alginate, there is always the risk of releasing cells into the environment. Therefore, alginate gels are impractical for field applications due to their inferior mechanical properties, inability to stop cell leakage, and poor cell viability during storage (Vancov et al., 2005). A very recent study reported encapsulation of *Pseudomonas* sp. ADP cells into core/shell nanofibers for atrazine bioremediation (Klein et al., 2012). The cell suspension was mixed with a core solution of polyethylene oxide dissolved in water, which was electrospun with a shell solution made of polycaprolactone and polyethylene glycol dissolved in chloroform and dimethylformamide. The atrazine degradation rate was reported as 0.0023 μmol/g of nanofibers/min following bioencapsulation. Although atrazine degradation was restored to 0.039 μmol/g of nanofibers/min by allowing the cells to grow in the nanofibers, the degradation rate of the encapsulated cells was still an order of magnitude less than the free cells. It is probable that the organic solvents involved in electrospinning had adverse effects on the enzymatic pathway for atrazine bioremediation.

In this study, atrazine degradation activity of both free *E. coli* expressing AtzA and nanofiber encapsulated *E. coli* expressing AtzA were assessed using HPLC analysis. In order to measure the reaction rates and the bioremediation efficiency accurately, the measurements focused on production of hydroxyatrazine in order to eliminate the bias due to adsorption of atrazine by silica (Reátegui et al., 2012). Table IV shows the quantities of atrazine degraded/adsorbed and hydroxyatrazine produced per unit gram of *E. coli* (or per gram of nanofibers) per minute for free and encapsulated *E. coli*. In both cases, the rate of atrazine degraded or adsorbed was comparable to that of hydroxyatrazine produced, implying that adsorption of atrazine into the silica-based nanofibers was negligible. The specific activity of the encapsulated *E. coli* was at the same order of magnitude as that of the free *E. coli*, indicating that the optimized reactive membranes did not present significant diffusional resistance.

We showed that we could achieve high degradation activity levels in electrospun reactive filters that are comparable to free-cells. In a novel approach, a multilayer geometry was utilized and the bacterium-containing core was enveloped in a porous shell produced in a continuous fashion. This served the purpose of increasing the biocompatibility of the process, adding an extra layer of separation between the bacteria and the environment (to further protect against accidental release) and also enhanced the encapsulation efficiency while minimizing the diffusion length. This scalable technology can be used to manufacture bioreactive filters that can biodegrade chemicals at large throughput levels, replacing the traditional size exclusion-based filtration systems. This opens new

Table IV. Biotransformation of atrazine into hydroxyatrazine.

	Free *E. coli* expressing AtzA	Encapsulated *E. coli* expressing AtzA
Mole of atrazine degraded or adsorbed (μmol/g of *E. coli*/min)	0.64	0.24
Mole of atrazine degraded or adsorbed (μmol/g of nanofibers/min)	N/A	0.10
Mole of hydroxyatrazine produced (μmol/g of *E. coli*/min)	0.61	0.23
Mole of hydroxyatrazine produced (μmol/g of nanofibers/min)	N/A	0.10

avenues in industrial scale bioremediation of contaminated waters.

Conclusions

Reactive membranes comprising electrospun nanofibers composed of a PVA core that encapsulate reactive *E. coli* and a silica/PVA composite shell surrounding this core were fabricated by a novel coaxial electrospinning method. Using this method, a very high loading efficiency of up to 40 g of *E. coli* in 100 g of matrix material could be reached. The atrazine biodegradation rate achieved by the reactive membranes produced by this method was quite high at 0.24 μmol/g of *E. coli*/min, which is approximately 40% that of the free bacteria (0.64 μmol/g of *E. coli*/min).

We acknowledge the support of an NSF-IIP/PFI grant (#1237754), an NSF-CAREER award (#0644784), and seed and fellowship grants from the BioTechnology Institute and the College of Biological Sciences in University of Minnesota. The authors thank Mr. Alan Twomey, Ms. Lisa Kasinkas, Ms. Lisa Strong, and Ms. Sujin Yeom for their help during the experimental work.

References

Abbasizadeh S, Keshtkar AR, Mousavian MA. 2013. Preparation of a novel electrospun polyvinyl alcohol/titanium oxide nanofiber adsorbent modified with mercapto groups for uranium(VI) and thorium(IV) removal from aqueous solution. Chem Eng J 220:161–171.

Bhardwaj N, Kundu SC. 2010. Electrospinning: A fascinating fiber fabrication technique. Biotechnol Adv 28:325–347.

Dai Y, Niu J, Yin L, Xu J, Xu J. 2013. Laccase-carrying electrospun fibrous membrane for the removal of polycyclic aromatic hydrocarbons from contaminated water. Sep Purif Technol 104:1–8.

de Souza ML, Wackett LP, Boundy-Mills KL, Mandelbaum RT, Sadowsky MJ. 1995. Cloning, characterization, and expression of a gene region from *Pseudomonas* sp. strain ADP involved in the dechlorination of atrazine. Appl Environ Microbiol 61(9):3373–3378.

Fung WY, Yuen KH, Liong MT. 2011. Agrowaste-based nanofibers as a probiotic encapsulant: Fabrication and characterization. J Agric Food Chem 59(15):8140–8147.

Gensheimer M, Becker M, Brandis-Heep A, Wendorff JH, Thauer RK, Greiner A. 2007. Novel biohybrid materials by electrospinning: Nanofibers of poly(ethylene oxide) and living bacteria. Adv Mater 19(18):2480–2482.

Guillette LJ, Iguchi T. 2012. Life in a contaminated world. Science 337(6102):1614–1615.

Irani M, Keshtkar AR, Moosavian MA. 2012. Removal of cadmium from aqueous solution using mesoporous PVA/TEOS/APTES composite nanofiber prepared by sol–gel/electrospinning. Chem Eng J 200–202:192–201.

Katoch A, Kim SS. 2012. Synthesis of hollow silica fibers with porous walls by coaxial electrospinning method. J Am Ceramic Soc 95(2):553–556.

Kim Y-J, Ahn CH, Choi MO. 2010. Effect of thermal treatment on the characteristics of electrospun PVDF-silica composite nanofibrous membrane. Eur Polym J 46(10):1957–1965.

Klein S, Kuhn J, Avrahami R, Tarre S, Beliavski M, Green M, Zussman E. 2009. Encapsulation of bacterial cells in electrospun microtubes. Biomacromolecules 10(7):1751–1756.

Klein S, Avrahami R, Zussman E, Beliavski M, Tarre S, Green M. 2012. Encapsulation of *Pseudomonas* sp. ADP cells in electrospun microtubes for atrazine bioremediation. J Ind Microbiol Biotechnol 39(11):1605–1613.

Li S, Yue X, Jing Y, Bai S, Dai Z. 2011. Fabrication of zonal thiol-functionalized silica nanofibers for removal of heavy metal ions from wastewater. Colloids Surf A 380(1–3):229–233.

Liu Y, Rafailovich MH, Malal R, Cohn D, Chidambaram D. 2009. Engineering of bio-hybrid materials by electrospinning polymer-microbe fibers. Proc Natl Acad Sci 106(34):14201–14206.

Lopez-Rubio A, Sanchez E, Sanz Y, Lagaron JM. 2009. Encapsulation of living bifidobacteria in ultrathin PVOH electrospun fibers. Biomacromolecules 10(10):2823–2829.

Lopez-Rubio A, Sanchez E, Wilkanowicz S, Sanz Y, Lagaron JM. 2012. Electrospinning as a useful technique for the encapsulation of living bifidobacteria in food hydrocolloids. Food Hydrocolloids 28(1):159–167.

Ma Z, Ji H, Teng Y, Dong G, Zhou J, Tan D, Qiu J. 2011. Engineering and optimization of nano- and mesoporous silica fibers using sol–gel and electrospinning techniques for sorption of heavy metal ions. J Colloid Interf Sci 358(2):547–553.

Mahapatra A, Mishra BG, Hota G. 2012. Studies on electrospun alumina nanofibers for the removal of chromium(VI) and fluoride toxic ions from an aqueous system. Ind Eng Chem Res 52(4):1554–1561.

Miao J, Miyauchi M, Simmons TJ, Dordick JS, Linhardt RJ. 2010. Electrospinning of nanomaterials and applications in electronic components and devices. J Nanosci Nanotechnol 10:5507–5519.

Moghe AK, Gupta BS. 2008. Co-axial electrospinning for nanofiber structures: Preparation and applications. Polym Rev 48(2):353–377.

Nassif N, Bouvet O, Noelle Rager M, Roux C, Coradin T, Livage J. 2002. Living bacteria in silica gels. Nat Mater 1(1):42–44.

Niu J, Dai Y, Guo H, Xu J, Shen Z. 2013a. Adsorption and transformation of PAHs from water by a laccase-loading spider-type reactor. J Hazard Mater 248–249:254–260.

Niu J, Xu J, Dai Y, Xu J, Guo H, Sun K, Liu R. 2013b. Immobilization of horseradish peroxidase by electrospun fibrous membranes for adsorption and degradation of pentachlorophenol in water. J Hazard Mater 246–247:119–125.

Patel AC, Li S, Yuan J-M, Wei Y. 2006. In situ encapsulation of horseradish peroxidase in electrospun porous silica fibers for potential biosensor applications. Nano Lett 6(5):1042–1046.

Pelton JT, McLean LR. 2000. Spectroscopic methods for analysis of protein secondary structure. Anal Biochem 277(2):167–176.

Pirzada T, Arvidson SA, Saquing CD, Shah SS, Khan SA. 2012. Hybrid silica-PVA nanofibers via sol–gel electrospinning. Langmuir 28(13):5834–5844.

Ponton A, Warlus S, Griesmar P. 2002. Rheological study of the sol–gel transition in silica alkoxides. J Colloid Interf Sci 249(1):209–216.

Reátegui E, Reynolds E, Kasinkas L, Aggarwal A, Sadowsky M, Aksan A, Wackett L. 2012. Silica gel-encapsulated AtzA biocatalyst for atrazine biodegradation. Appl Microbiol Biotechnol 96(1):231–240.

Reznik SN, Yarin AL, Zussman E, Bercovici L. 2006. Evolution of a compound droplet attached to a core–shell nozzle under the action of a strong electric field. Phys Fluids 18(6):062101.

Rietti-Shati M, Ronen D, Mandelbaum RT. 1996. Atrazine degradation by *Pseudomonas* strain ADP entrapped in sol–gel glass. J Sol–Gel Sci Technol 7:77–79.

Salalha W, Kuhn J, Dror Y, Zussman E. 2006. Encapsulation of bacteria and viruses in electrospun nanofibres. Nanotechnology 17(18):4675–4681.

Schwarzenbach RP, Escher BI, Fenner K, Hofstetter TB, Johnson CA, von Gunten U, Wehrli B. 2006. The challenge of micropollutants in aquatic systems. Science 313(5790):1072–1077.

Shin K-H, Sung J-H, Koh Y-H, Lee J-H, Choi W-Y, Kim H-E. 2010. Direct coating of bioactive sol–gel derived silica on poly(ε-caprolactone) nanofibrous scaffold using co-electrospinning. Mater Lett 64(13):1539–1542.

Singh P, Mondal K, Sharma A. 2013. Reusable electrospun mesoporous ZnO nanofiber mats for photocatalytic degradation of polycyclic aromatic hydrocarbon dyes in wastewater. J Colloid Interf Sci 394: 208–215.

Strong LC, McTavish H, Sadowsky MJ, Wackett LP. 2000. Field-scale remediation of atrazine-contaminated soil using recombinant *Escherichia coli* expressing atrazine chlorohydrolase. Environ Microbiol 2(1):91–98.

Tsou PH, Chou CK, Saldana SM, Hung MC, Kameoka J. 2008. The fabrication and testing of electrospun silica nanofiber membranes for the detection of proteins. Nanotechnology 19(44):445714.

Vancov T, Jury K, van Zwieten L. 2005. Atrazine degradation by encapsulated *Rhodococcus erythropolis* NI886/21. J Appl Microbiol 99:767–775.

Wang F, Ge M. 2013. Fibrous mat of chitosan/polyvinyl alcohol/containing cerium(III) for the removal of chromium(VI) from aqueous solution. Text Res J 83(6):628–637.

Wang Z-G, Wan L-S, Liu Z-M, Huang X-J, Xu Z-K. 2009. Enzyme immobilization on electrospun polymer nanofibers: An overview. J Mol Catal B 56(4):189–195.

Zucchelli A, Focarete ML, Gualandi C, Ramakrishna S. 2011. Electrospun nanofibers for enhancing structural performance of composite materials. Polym Adv Technol 22(3):339–349.

Zussman E. 2011. Encapsulation of cells within electrospun fibers. Polym Adv Technol 22(3):366–371.

Supporting Information

Additional supporting information may be found in the online version of this article at the publisher's web-site.